RSC Advances

PAPER

View Article Online
View Journal | View Issue

Cite this: *RSC Adv.*, 2021, **11**, 32565

A thermoreversible crosslinking hot-melt adhesive: reversibility and performance

Wang Xiangjun,[ab] Xinzhong Li,[ab] Qi Lin,[ab] Jianrong Xia *[ab] and Hanyu Xue *[ab]

Received 10th July 2021
Accepted 17th September 2021

DOI: 10.1039/d1ra05319a

rsc.li/rsc-advances

The need to improve the environmental friendliness and achieve the recycling of resins is an ongoing process for hot-melt adhesive technology. In this work, a new type of thermoreversible crosslinking hot-melt adhesive-based Diels Alder (DA) reaction was prepared. The critical idea was to efficiently initiate the esterification to yield furoic acid (FA)-grafted poly(vinyl alcohol) (PVA-*g*-FA), and then PVA-*g*-FA was mixed with *N*,*N*′-(4,4′-methylenediphenyl)dimaleimide (MDI) to finally obtain the thermoreversible crosslinking adhesive (PVA-*g*-FA/MDI). The experimental results indicated that the reversibility of the DA reaction between the furan rings and the maleimide groups allowed PVA-*g*-FA/MDI to be dynamically crosslinked. It was able to crosslink at a temperature of 80 °C and decrosslink at 120 °C. Moreover, the performances of hot-melt adhesive were investigated. The PVA-*g*-FA/MDI had a better peeling strength (43.33 N mm^{-1}), bond strength (11.84 MPa), and thermal conductivity (0.263 W m^{-1} K^{-1}) than PVA resins. The light-transmittance and haze value were 52.8% and 12.24‰, respectively. The PVA-*g*-FA/MDI resin could be reused more than two times.

1. Introduction

Heat-seal adhesives (HSAs) are widely used in all aspects of life, such as textiles, furniture, home appliances, cultural relics protection, packaging and medical consumables.[1–5] The existing thermoplastic and thermoset HSAs have certain shortcomings. The adhesion strength and solvent resistance of thermoplastic-HMAs are relatively poor owing to their linear structure. Thermoset-HMAs are non-reworkable and unrecyclable with low initial adhesion strength. Thermoset-HMAs are a popular choice of adhesives on account of their high performance, durability and versatility.[6] However, irreversibly crosslinked polymer networks do not facilitate the re-use or recycling of materials.

There was a growing interest in the re-use or recycling of HMAs, which comprise chemical crosslinks that were dynamic under specific stimuli, potentially enabling recyclability. These dynamic crosslinking bonds included transesterification using ester/hydroxyl groups,[7,8] transesterification using boronic esters,[9] the dynamic exchange of thioesters with thiols,[10,11] and others.[12–17] However, while these recyclable adhesives were recyclable and degradable, their heat resistance and mechanical properties were reduced. For example, the former are unstable after 1 hour at 90 °C due to side reactions, whereas the latter are unstable above 120 °C due to thioester decomposition.[9]

The (retro-) Diel–Alder reaction (DA reaction) between the maleimide and furan groups had been used in the re-use or recycling of HMAs. For example, L. M. Sridhar[6] synthesized maleimide-functional telechelic prepolymers and polyfunctional furan crosslinkers *via* facile techniques. Then, they were mixed with solvent-free polyester and poly(ester urethane) at moderate temperatures to prepare reusable HSAs. The reusable HSAs were shown to be thermally stable up to 150 °C. The adhesive and bonded substrates could be re-used repeatedly without the use of solvents. M. Y. Wu[18] synthesized a polyurethane hot-melt adhesive (CDI-PUR-DA) *via* the introduction of a thermally reversible covalent Diels–Alder adduct into the polyurethane main chain. CDI-PUR-DA also exhibited good adhesive properties even after 3 times adhesion. In the study of appeal, the Diels–Alder functional groups were involved in the resin in the form of monomers or end groups. As a result, most of the reusable HSAs were linear products with uncontrollable molecular weight, poor mechanical properties, heat resistance and solvent resistance. Therefore, the development of new HSAs with high molecular weight and intermolecular reversible crosslinking had become a hot spot.

Traditional hot-melt adhesives such as ethylene vinyl acetate (EVA) are based upon thermoplastic resins, which could be cured by peroxide initiators to form thermoset HSAs. After curing, the mechanical properties and heat resistance of EVA were greatly improved. Inspired by EVA HSAs and DA reaction,[19–21] we designed a new thermoreversible crosslinked hot-melt adhesive. The critical idea was to create a DA derivative-based thermoreversible crosslinked resin by taking poly(vinyl alcohol) macromolecular resin as a matrix, and introducing

[a]*Fujian Engineering and Research Center of New Chinese Lacquer Materials, Ocean College, Minjiang University, Fuzhou, Fujian 350108, P. R. China. E-mail: jrxia@mju.edu.cn; 366157115@qq.com*

[b]*Fujian Provincial University Engineering Research Center of Green Materials and Chemical Engineering, Minjiang University, Fuzhou, Fujian 350108, P. R. China*

functional groups into the side chain as crosslinking points.[22,23] The developed thermoreversible crosslinked hot-melt adhesive could be reused, and the adhesive exhibits excellent thermo and mechanical properties.

2. Experimental section

2.1 Materials and reagents

Poly(vinyl alcohol)-1799 (PVA-1799, alcoholysis degree 98–99%), furoic acid (FA, AR, 99%), ditin butyl dilaurate (DBD, CP, 95%), *N*,*N*′-dimethyformamide (DMF, AR, 99%), *N*,*N*′-dicyclohexycarbodiimide (DCCD, AR, 99%) and ethyl acetate (AR, 99%) were purchased from Aladdin Chemical Reagent Co, Ltd., Shanghai, China. *N*,*N*′-(4,4′-Methylenediphenyl)dimaleimide (MDI, AR, 99.0%) was supplied by Honghu City Shuangma New Material tch Co., Ltd (China).

2.2 Synthesis of PVA-*g*-FA

PVA-*g*-FA was synthesized by the esterification reaction (Scheme 1). PVA (5.0 g) was completely dissolved in 50 mL DMF at 120 °C in a 150 mL three-neck round-bottom flask. After cooling down to 100 °C, FA (5.0 g) and *N*,*N*′-dicyclohexycarbodiimide (1.0 mL, as dehydrating agent) were added under stirring. Then, the catalyst di-butyl dilaurate was added dropwise into the flask. The reaction lasted for 24 h at 88 °C under a nitrogen atmosphere. The excess solvent was removed by a rotary evaporator. Finally, the raw product (light brown viscous liquid) was extracted and purified by ethyl acetate, and dried in a vacuum at 60 °C for 24 h.

2.3 Preparation of the PVA-FA/MDI resins

PVA-*g*-FA was completely dissolved in 50.0 mL DMF at 100 °C in a 150 mL three-neck round-bottom flask. Then, the MDI was added under stirring. The mixing lasted for 0.5 h under a nitrogen atmosphere. The mixed solution was poured into a silicone mold. The excess solvent was removed by a rotary evaporator. Finally, the product was extracted and purified by ethyl acetate, and dried in a vacuum at 60 °C for 24 h.

2.4 Characterizations

Samples of PVA and PVA-*g*-FA/MDI were prepared in the form of a film (0.20 mm thick). A ThermoFisher IS10 Fourier transformation infrared spectrometer was used to record Fourier transform infrared (FT-IR) spectra. The spectra were obtained in the range of 4000–525 cm^{-1}. The number of scans was 32 at the resolution of 2 cm^{-1}. ^1H NMR spectra of the samples were measured by a VARIAN Mercury-Plus 300 (300 MHz) with dimethyl sulfoxide (DMSO-d_6) as the solvent. Differential scanning calorimetry (DSC) measurements were performed on a TA Instruments DSC 2500 (at a heating rate of 10 °C min^{-1}, a nitrogen purge, and an empty aluminum pan as the reference). Thermogravimetric analysis was examined by a TA Instruments DSC 2500 (at a heating rate of 10 °C min^{-1}, nitrogen purge) and using a nitrogen purge.

To trace the thermoreversible crosslinking reaction of PVA-*g*-FA/MDI, the gel contents (CR%) of the PVA-*g*-FA/MDI resin were tested by DMF extraction method (technically equivalent to the standard ISO 16152 and ASTM D5492), and calculated according to the following eqn (1):

$$GC\% = (W_1 - W_2)/W_1 \times 100\% \quad (1)$$

In the equation, W_1 was the weight of the PVA-*g*-FA/MDI resin before extraction, and W_2 was the weight of the resin after extraction.

For a quantitative description of the performance for the hot-melt adhesive, (1) the adhesion strength of the PVA-*g*-FA/MDI resin in the glass/resin system was performed on a universal testing machine, model H10K-S (Hounsfield, the United Kingdom) according to ISO 8510-2 at a crosshead speed of 5 cm min^{-1}. Each value obtained represented the average of nine samples. (2) To determine the bond strength of the PVA adhesive samples, the dry adhesive strength of the PVA samples was determined using block shear tests of the dry glued samples according to ASTM D905-98. (3) The light transmittance and haze value of the light reversible crosslinking resin were tested on a transmittance haze meter, model LH-206 (China) according to ASTM D-1003. (4) The thermal conductivity was tested by a thermal conductivity tester (DRM-2, China). The sample size was at least 20 mm × 20 mm × 3 mm. (5) The electrical insulation properties of resin were tested by a high-resistance meter (Agilent 4339B, United States of America). The sample size was at least 20 mm × 20 mm × 3 mm. The wide measurement range was 10^3 Ω cm^{-1} to 1.6 × 10^{16} Ω cm^{-1} with a 10 ms high-speed measurement.

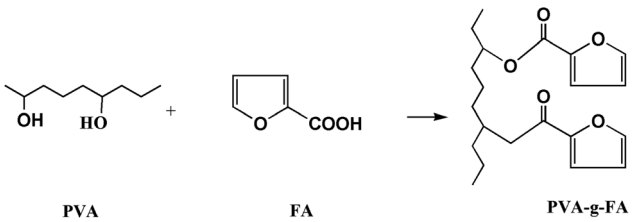

Scheme 1 Synthesis of PVA-*g*-FA.

3. Results and discussion

3.1 Synthesis of PVA-*g*-FA

PVA-*g*-FA was synthesized by esterification reaction under the catalysis of dith-butyl dilaurate. FTIR and ^1H NMR measurements were used to confirm the esterification graft reaction. The FTIR spectra For PVA are shown in Fig. 1a. The two peaks at 1459 and 1333 cm^{-1} suggested the presence of –CH_2 in the backbone. The peaks at 2927 and 2838 cm^{-1} represented –CH_2 in the backbone stretching vibrations absorption. In addition, the peak at 3329 cm^{-1} represented the –OH group in the backbone stretching vibrations absorption. For PVA-*g*-FA (Fig. 1b), the most striking difference with the PVA sample was the appearance of a peak at 1711 cm^{-1}, which represented the ester C=O absorption (including the contribution of a conjugative effect of phenyl), and that at 1661 cm^{-1} was related to

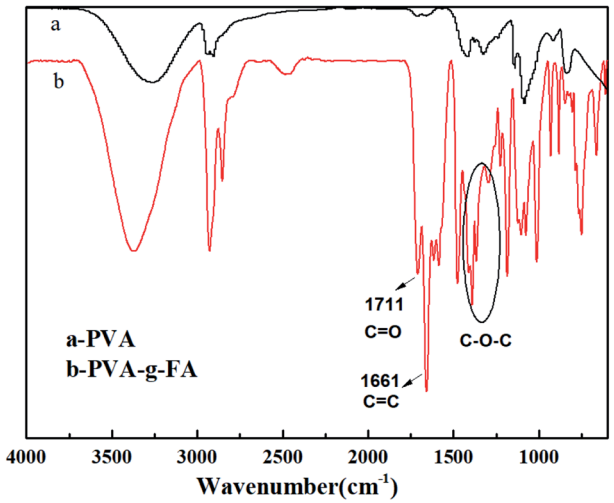

Fig. 1 FTIR spectra of PVA and PVA-*g*-FA.

the C=C of phenyl absorption. The peaks at 1380, 1182 and 1107 cm^{-1} represented the C–O–C absorption in the furan group of PVA-*g*-FA. The changes in the FTIR spectra proved that PVA-*g*-FA was synthesized successfully by esterification reaction.[24–27]

^{1}H NMR measurements were conducted to further investigate the synthesis of PVA-*g*-FA. The results of the ^{1}H NMR measurements are shown in Fig. 2. As shown in Fig. 2a, the protons of the PVA backbone were correlated to peaks at 1.20, 1.23, 1.30 and 1.45 ppm, the protons of $-CH_2$-OH were assigned to peaks at 3.33 ppm, and the protons of –OH were observed at 2.48 ppm. For the samples, the protons of the furan rings in FA (Fig. 2b) were related to peaks at 6.61, 7.16 and 7.88 ppm, while the protons of the carbonyl were observed at 11.10 ppm. For the samples of PVA-*g*-FA, characteristic peaks of FA (such as protons of aromatic rings at 6.39, 7.08 and 7.91 ppm) were found in the ^{1}H NMR spectra of PVA-*g*-FA. Therefore, a conclusion could be drawn that PVA-*g*-FA was synthesized successfully by esterification reaction under the catalysis of dith-butyl dilaurate.[22–25]

3.2 Thermo analysis

Fig. 3 presents the TG experimental results of PVA and PVA-*g*-FA. For PVA (a), which had the best thermal stability, its initial decomposition temperature (IDT) was about 230 °C. A significant mass loss occurred within the temperature range of 230–350 °C with a mass loss rate of 82.2%. This decomposition was due to the pyrolysis of PVA. The weight loss observed in this temperature range was related to some volatile products, such as carbon dioxide, other lower aldehydes and ketones.[23] For PVA-*g*-FA (e), the IDT was about 200 °C and a significant mass loss occurs within the temperature range of 200–375 °C with a mass loss ester group and backbone in PVA-*g*-FA. The

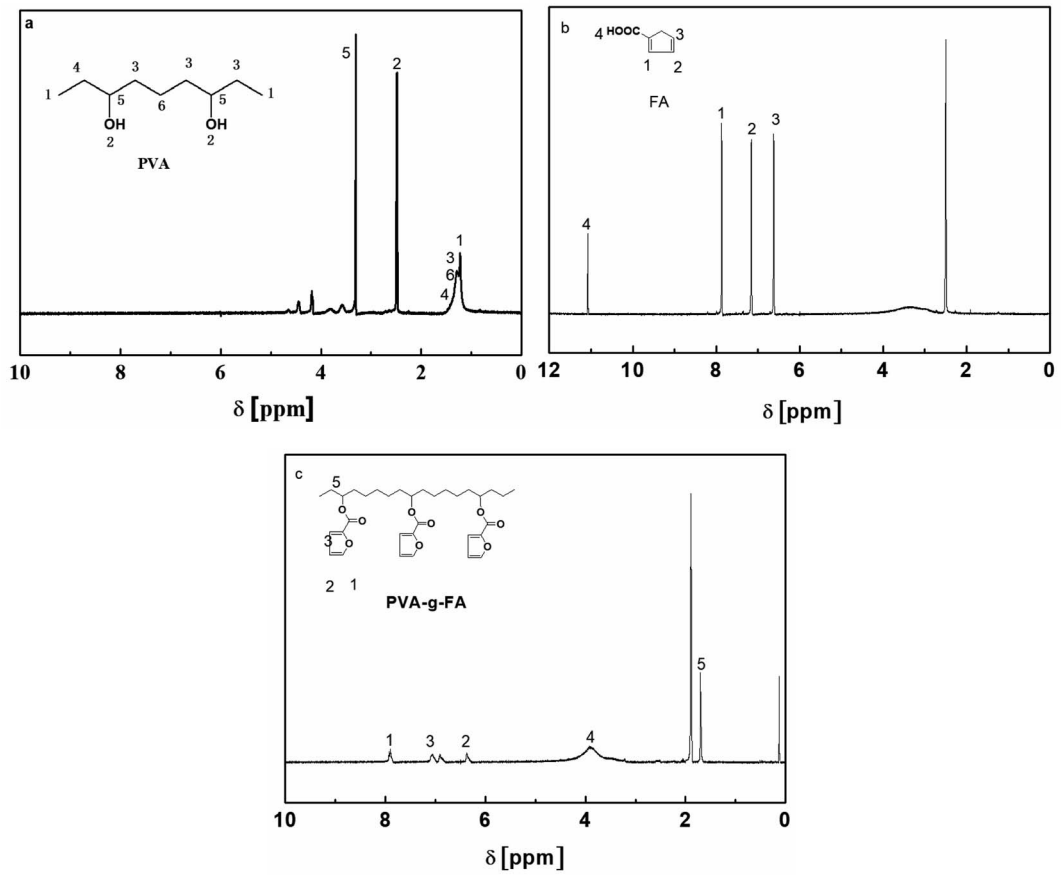

Fig. 2 ^{1}H NMR spectra of PVA (a), FA (b) and PVA-*g*-FA (c).

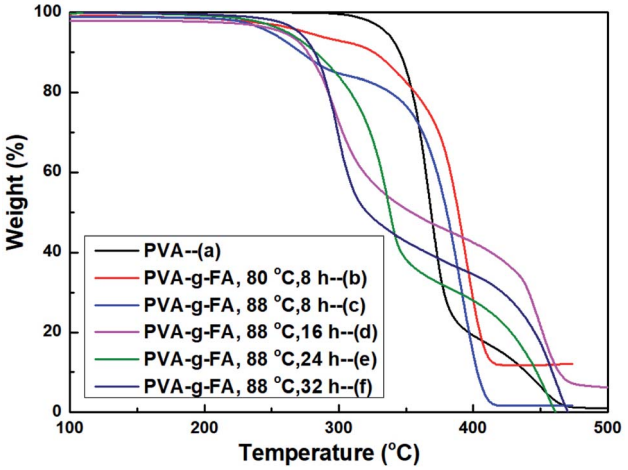

Fig. 3 TG curves of PVA and PVA-*g*-FA.

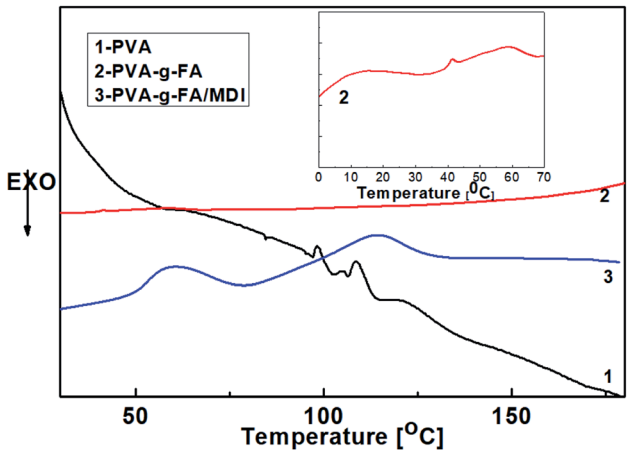

Fig. 4 DSC curves of PVA, PVA-*g*-FA and PVA-*g*-FA/MDI.

decomposition temperature of the ester group was generally lower than 300 °C. It was the pyrolysis of the ester group between 265–300 °C. The weight loss rate, that was, the grafting rate of PVA-*g*-FA, was 34%. Then, the decomposition of the ethylene unit and ungrafted vinyl acetate unit occurs within the temperature range of 375–488 °C. TG analysis showed that PVA-*g*-FA was thermally stable up to 265 °C. This behaviour far exceeds the thermal stability reported for epoxy adhesives from Diels–Alder networks comprising maleimide/furan functional groups[28] and acrylic polymers from hetero-Diels–Alder networks based on thioesters.[29]

In addition, the grafting reaction of the resin was optimized by TG analysis. It could be seen from Fig. 3 that the lower temperature (at 80 °C, Fig. 3b) was not conducive to the grafting reaction. The grafting rate of the resin was improved by increasing the temperature to 88 °C and prolonging the reaction time. The highest grafting rate was 34% at 88 °C and 24 hours (Fig. 3e). Further prolonging the reaction time aggravates the reverse reaction, and reduces the grafting rate (Fig. 3f). Higher grafting rate means higher crosslinking degree. Therefore, we could optimize the best grafting reaction conditions (as show in 2.2. Synthesis of PVA-*g*-FA).

The DSC melting endotherms corresponding to the second heating scans for PVA and PVA-*g*-FA are shown in Fig. 4. Concerning the second heating scan of PVA, the melting endotherms occurred at 100–110 °C with an endothermic peak. This phenomenon was caused by strong hydrogen bond interactions, both inter and intra-molecular, as well as successive self-nucleation, which reduced the free volume of the polymer chains. For a sample of PVA-*g*-FA, the melting endotherms at 100–110 °C disappeared, and were replaced by an endothermic peak at about 60 °C and an endothermic platform at about 0–10 °C. These correspond to the melting temperature and glass transition temperature of PVA-*g*-FA, respectively, indicating that FA was grafted into the backbone of PVA successfully. For a sample of PVA-*g*-FA/MDI, the DSC curves showed a completely different trend. There was an exotherm peak at 80 °C that appeared after the melting endothermic peak of PVA-*g*-FA at 60 °C, implying the crosslinking of PVA-*g*-FA/MDI. Simultaneously, an endothermic peak at 120 °C indicated the decrosslinking of PVA-*g*-FA/MDI. Therefore, the conditions of thermo-reversible crosslinking reactions (Scheme 2) could be optimized with the temperature of crosslinking at 80 °C and the temperature of decrosslinking at 120 °C.[22–25]

In order to further optimize the conditions of the thermo-reversible crosslinking reaction, the gel content of the samples was calculated by *N*,*N*-dimethylformamide (DMF) extraction method. Table 1 shows the influence of the *N*,*N*′-4,4′-diphenylmethane bismaleimide (MDI) amount on the gel content of PVA-*g*-FA/MDI. It could be seen from the table that the gel contents of the PVA-*g*-FA/MDI resin increase with the content of MDI. When the ratio of PVA-*g*-FA : MDI was 2.0 g : 0.4 g, the gel content of the resin reached a maximum of 83.2%. Then, the gel content of the resin decreased with increasing MDI. Therefore, the optimal ratio of PVA-*g*-FA : MDI was 2.0 g : 0.4 g.

Table 2 shows the gel contents of PVA-*g*-FA/MDI, which showed a trend of increasing with crosslinking time under 80 °C. When the crosslinking time was 1 h, the gel content of the PVA-*g*-FA/MDI resin reached a maximum of 82.1%. Because the thermoreversible crosslinking was partially reversible,[30–33] after decrosslinking at 120 °C for 2 h, a portion of the PVA-FA/MDI resin was converted into the linear polymer. The gel content of the PVA-*g*-FA/MDI resin was reduced to approximately 4.3%. In summary, the optimal condition of the thermoreversible crosslinking reaction was PVA-*g*-FA : MDI of 2.0 g : 0.4 g and a crosslinking time of 2 h at 80 °C.

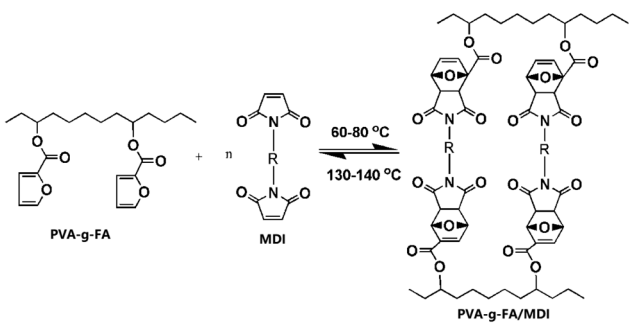

Scheme 2 Thermo-reversible crosslinking reaction of PVA-FA/MDI.

Table 1 The influence of the MDI content on the gel content of PVA-*g*-FA/MDI

PVA-*g*-FA : MDI	Gel content of PVA-*g*-FA/MDI crosslinked at 80 °C	Gel content of PVA-*g*-FA/MDI decrosslinked at 120 °C
2.0 g : 0.2 g	65.9% (±1.20%)	3.2% (±0.22%)
2.0 g : 0.4 g	82.2% (±0.81%)	5.4% (±0.14%)
2.0 g : 0.6 g	74.2% (±0.52%)	4.3% (±0.17%)
2.0 g : 0.8 g	72.1% (±0.66%)	4.1% (±0.25%)
2.0 g : 1.0 g	62.9% (±0.83%)	3.6% (±0.24%)

Table 2 The influence of the curing time for the gel content of PVA-*g*-FA/MDI

PVA-*g*-FA/MDI (2.0 g:0.4 g)	0.5 h	1 h	1.5 h	2 h	2.5 h	3 h
Gel content of PVA-*g*-FA/MDI crosslinked at 80 °C	65.3% (±0.98%)	73.6% (±0.65%)	77.5% (±0.73%)	82.1% (±0.68%)	81.9% (±0.85%)	81.2% (±0.75%)
Gel content of PVA-*g*-FA/MDI decrosslinked at 120 °C	3.2% (±0.33%)	3.9% (±0.27%)	4.2% (±0.18%)	4.3% (±0.22%)	4.4% (±0.11%)	4.3% (±0.32%)

3.3 Reusability

The reusability of PVA-*g*-FA/MDI was also tested by extraction method. The DMF extraction results of the PVA-*g*-FA/MDI samples of different reuse times are shown in Table 3. It could be seen from Table 3 that PVA-*g*-FA/MDI undergoes crosslinking after heating at 80 °C, and the crosslinking degree of the sample was 82.1%. When the recovered samples were used for the first time, the degree of cross-linking drops to 73.2%. These values were reduced to 70.4% and 63.1% for the samples used for the second time and third time, respectively. If the critical service condition was 70% crosslinking degree, the crosslinking degree of the resin decreased greatly after being reused twice, which needs further improvement.

3.4 Adhesive performance

The bonding property was one of the most important properties of the heat-seal adhesive,[26] which could be directly reflected by the peel strength.[27] For samples of PVA-*g*-FA/MDI, the peel strength increased to 43.33 N mm^{-1}, which was 94.8% higher than that of PVA (Table 4). This bond strength was higher than that of the modified PVA recorded in the relevant literature (10.3 MPa),[34] and is also significantly higher than that of similar reversible crosslinking hot-melt adhesives (7.3 MPa).[18]

The bond strength increased to 11.84 MPa, which was 49.5% higher than that of PVA (Table 5). The improvement of adhesion could be attributed to the high polarity of PVA-*g*-FA/MDI. The furyl groups that were grafted into the molecular chain, as well as MDI, lead PVA-*g*-FA/MDI to a stronger polar polymer (Fig. 5).[26,27] It is shown in Fig. 4 that the contact angle of PVA with water was 90.50° and 32.53° with diiodomethane. The contact angles of PVA-*g*-FA/MDI decreased to 25.34° with water and 37.72° with diiodomethane.

To verify the analysis from the viewpoint of thermodynamics, the surface energies, γ, of the related materials were measured, in which γ_d and γ_p represent the dispersion and polar parts, respectively.[21] Accordingly, the work of adhesion, W, can be calculated from:

$$W_{AB} = 2\sqrt{\gamma_A^d \gamma_B^d} + 2\sqrt{\gamma_A^p \gamma_B^p} \quad (2)$$

where the subscripts A and B denote the material pairs in contact. From the data in Table 6, the work of adhesion between glass and PVA was 79.1 mJ m^{-2}, while the work of adhesion between glass and PVA-*g*-FA/MDI was 101.6 mJ m^{-2}. Evidently, a large amount of energy was consumed when breaking the

Table 4 Peeling strength of PVA and PVA-*g*-FA/MDI

Sample	Mean (N mm^{-1})	Std. deviation (%)
PVA	23.22	0.89275
PVA-*g*-FA/MDI	43.33	1.04403

Table 3 Crosslinking degree of the reused PVA-*g*-FA/MDI

	Reused times			
PVA-*g*-FA/MDI (2.0 g : 0.4 g)	0	1	2	3
Crosslinking degree (%)	82.1 (±0.61%)	73.2 (±0.46%)	70.4 (±0.58%)	63.1 (±0.87%)
Decrosslinking degree (%)	5.1 (±0.46%)	7.5 (±0.29%)	8.3 (±0.31%)	10.2 (±0.25%)

Table 5 Bond strength of PVA and PVA-*g*-FA/MDI

Sample	Mean (MPa)	Std. deviation (%)
PVA	7.92	0.76335
PVA-*g*-FA/MDI	11.84	0.89532

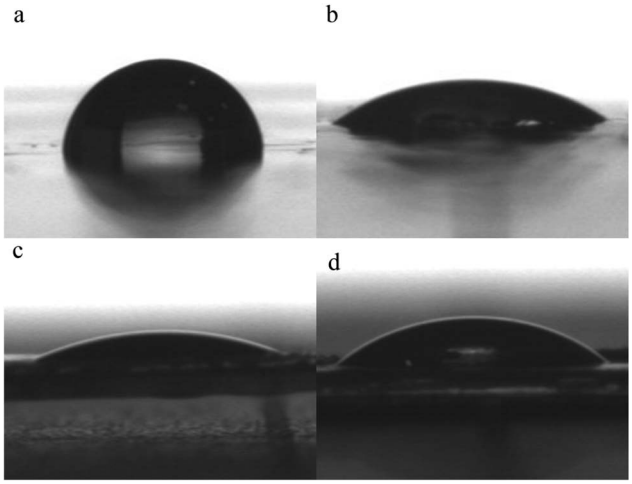

Fig. 5 Contact angle of (a) PVA with water; (b) PVA with diiodomethane; (c) PVA-*g*-FA/MDI with water; (d) PVA-*g*-FA/MDI with diiodomethane.

joint of glass/PVA-*g*-FA/MDI apart. This means that the resin provided good adhesion to the polar substrates.

3.5 Optical property

The light transmittance and haze value of PVA-*g*-FA, PVA-*g*-FA/MDI were tested and the results are shown in Table 7. For the sample of PVA-*g*-FA, the light transmittance and haze value were

Table 6 Components of the surface free energies of PVA and PVA-*g*-FA/MDI

Materials	γ (mJ m^{-2})	γ_d (mJ m^{-2})	γ_p (mJ m^{-2})
Glass	46.10	31.01	15.09
PVA	43.72	43.14	0.58
PVA-*g*-FA	59.32	24.92	34.40

Table 7 Light transmittance and haze value of PVA, PVA-*g*-FA and PVA-*g*-FA/MDI

Samples	PVA-*g*-FA	PVA-*g*-FA/MDI
Light transmittance (%)	56.9	52.8
Std. deviation (%)	1.12114	1.23318
Haze value (‰)	8.56	12.24
Std. deviation (%)	0.78823	0.84931

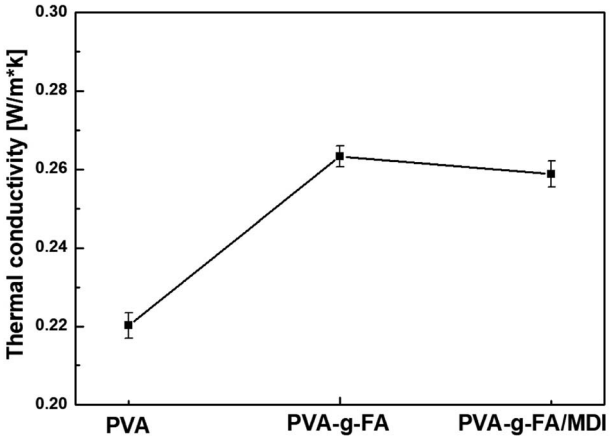

Fig. 6 Thermal conductivity of PVA and PVA-*g*-FA/MDI.

56.9% and 8.56‰, respectively. The light transmittance and haze value of PVA-*g*-FA/MDI decreased to 52.8%, and 12.24‰, respectively. This could be due to the grafted furyl group and added bismaleimide, which has a strong absorption of ultraviolet light, affecting the optical property of resins.

3.6 Thermal conductivity

Because hot-melt adhesives were widely used in electronic packaging, medical problems, and other applications, properties such as thermal conductivity and electrical insulation were very important for the heat-seal adhesive. Fig. 6 shows the thermal conductivity of therma-reversible crosslinked PVA-*g*-FA/MDI. The thermal conductivity of the PVA-*g*-FA/MDI resin was 0.263 W m^{-1} K^{-1}. In heat transfer, conduction (or heat conduction) was the transfer of thermal energy between regions of matter due to a temperature gradient. Heat always flows from a region of higher temperature to a region of lower temperature, and results in the elimination of temperature differences by establishing thermal equilibrium.[35,36] In solids, it is due to the combination of vibrations of the molecules in a lattice or phonons with the energy transported by free electrons. Side chains of furyl groups, which were considered as heat transfers, were grafted into the molecular chain of PVA-*g*-FA. However, it is difficult for the spaced-apart furyl groups to form an effective electron transmission channel. Thus, the thermal performance of PVA-*g*-FA/MDI improved, but it was difficult to achieve excellent thermal conductivity.

3.7 Electrical insulation property

Table 8 lists the bulk electrical resistivity of PVA and PVA-*g*-FA/MDI resin. For a sample of PVA, this value was 3.18 × 10^{15}

Table 8 Bulk electrical resistivity of PVA, PVA-*g*-FA and PVA-*g*-FA/MDI

Samples	Mean (Ω cm^{-1})	Std. deviation (%)
PVA	3.18	0.03911
PVA-*g*-FA/MDI	2.92	0.04225

Table 9 Tensile performance of PVA-*g*-FA/MDI

	Uncrosslinked PVA-*g*-FA/MDI		Crosslinked PVA-*g*-FA/MDI	
Samples	Mean	Std. deviation	Mean	Std. deviation
Tensile strength (MPa)	14.22	1.36	15.05	1.55

$\Omega\ cm^{-1}$. The bulk electrical resistivity of PVA-*g*-FA/MDI was $2.92 \times 10^{15}\ \Omega\ cm^{-1}$. This could be due to the introduction of a furyl group in the molecular chain. However, it was fortunate that the electrical insulation performance of PVA-*g*-FA still met the requirements of $10^{15}\ \Omega\ cm^{-1}$ for practical application.

3.8 Tensile performance

The tensile strengths of PVA-*g*-FA/MDI before and after crosslinking were compared. The test result was the average of five repeated tests. According to the test results in Table 9, the tensile strength of uncrosslinked PVA-*g*-FA/MDI was 14.22 MPa. Meanwhile, for the sample of crosslinked PVA-*g*-FA/MDI, the tensile strength was 15.05 MPa. This showed that PVA-*g*-FA/MDI had better mechanical properties. Crosslinking improved the mechanical properties of the resin.[37]

4. Conclusion

From the original intention of environmental protection, a new type of thermoreversible crosslinking hot-melt adhesive (PVA-*g*-FA/MDI) was prepared based on Diels–Alder reaction. Specifically, furoic acid (FA) was grafted into PVA successfully, and then mixed with MDI. The thermo-reversible crosslinking reaction was verified by DSC, showing that the resin was crosslinked at a temperature of 80 °C and decrosslinked at 120 °C. The optimal condition of the thermoreversible crosslinking reaction was PVA-*g*-FA : MDI of 2.0 g : 0.4 g and crosslinking time of 2 h at 80 °C. Performances of PVA-*g*-FA/MDI for the hot-melt adhesive were also investigated. Without any additives, PVA-*g*-FA/MDI had a better peeling strength (43.33 N mm^{-1}), bond strength (11.84 MPa), and thermal conductivity ($0.263\ W\ m^{-1}\ K^{-1}$) than PVA resins. The light-transmittance and haze value of PVA-*g*-FA/MDI are 52.8% and 12.24‰, respectively. The bulk electrical resistivity is $2.92 \times 10^{15}\ W\ cm^{-1}$. The tensile strength reaches 15.05 MPa. This research provides a new idea for exploring the recycling technology of the hot-melt adhesive.

Conflicts of interest

There are no conflicts to declare.

Acknowledgements

This work was financially supported by the National Natural Science Foundation of China (Grant No. 51703090), Fuzhou Municipal Science Foundation (Grant: 2020-GX-2), Fujian Provincial Natural Science Foundation (Grant: 2021J011019, 2021J011021), and Principal's Fund of Minjiang University (Grant: 103952020050).

References

1 R. H. Aguirresarobe, S. Nevejans, B. Reck, L. Irusta, H. Sardon, J. M. Asua and N. Ballard, Healable and self-healing polyurethanes using dynamic chemistry, *Prog. Polym. Sci.*, 2021, **114**, 101362, DOI: 10.1016/j.progpolymsci.2021.101362.

2 C. Ghobril and M. Grinstaff, The chemistry and engineering of polymeric hydrogel adhesives for wound closure: a tutorial, *Chem. Soc. Rev.*, 2015, **44**(7), 1820–1835, DOI: 10.1039/c4cs00332b.

3 C. Zhong, T. Gurry, A. A. Cheng, J. Downey, Z. Deng, C. M. Stultz and T. K. Lu, Strong underwater adhesives made by self-assembling multi-protein nanofibres, *Nat. Nanotechnol.*, 2014, **9**(10), 858–866, DOI: 10.1038/nnano.2014.199.

4 O. Pinkas, D. Goder, R. Noyvirt, S. Peleg, M. Kahlon and M. Zilberman, Structuring of composite hydrogel bioadhesives and its effect on properties and bonding mechanism, *Acta Biomater.*, 2017, **51**, 125–137, DOI: 10.1016/j.actbio.2017.01.047.

5 N. Annabi, Y. N. Zhang, A. Assmann, E. S. Sani, G. Cheng, A. D. Lassaletta, A. Vegh, B. Dehghani, G. U. Ruiz-Esparza, X. Wang, S. Gangadharan, A. S. Weiss and A. Khademhosseini, Engineering a highly elastic human protein-based sealant for surgical applications, *Sci. Transl. Med.*, 2017, **9**(410), 7466, DOI: 10.1126/scitranslmed.aai7466.

6 L. M. Sridhar, M. O. Oster, D. E. Herr, J. B. D. Gregg, J. A. Wilson and A. T. Slark, Re-usable thermally reversible crosslinked adhesives from robust polyester and poly(ester urethane) Diels–Alder networks, *Green Chem.*, 2020, **22**, 8669–8679, DOI: 10.1039/D0GC02938F.

7 D. Montarnal, M. Capelot, F. Tournilhac and L. Leibler, Silica-Like Malleable Materials from Permanent Organic, *Network Sci.*, 2011, **334**, 965–968, DOI: 10.1126/science.1212648.

8 W. Denissen, G. Rivero, R. Nicolaÿ, L. Leibler, J. M. Winne and F. E. Du Prez, Vinylogous Urethane Vitrimers, *Adv. Funct. Mater.*, 2015, **25**, 2451–2457, DOI: 10.1002/adfm.201404553.

9 W. Denissen, M. Droesbeke, R. Nicolaÿ, L. Leibler, J. M. Winne and F. E. Du Prez, Chemical control of the viscoelastic properties of vinylogous urethane vitrimers, *Nat. Commun.*, 2017, **8**, 14857, DOI: 10.1038/ncomms14857.

10 M. Röttger, T. Domenech, R. Van Der Weegen, A. Breuillac, R. Nicolaÿ and L. Leibler, High-performance vitrimers from commodity thermoplastics through dioxaborolane metathesis, *Science*, 2017, **356**, 62–65, DOI: 10.1126/science.aah5281.

11 B. T. Worrell, S. Mavila, C. Wang, T. M. Kontour, C. H. Lim, M. K. McBride, C. B. Musgrave, R. Shoemaker and C. N. Bowman, A user's guide to the thiol-thioester exchange in organic media: scope, limitations, and applications in material science, *Polym. Chem.*, 2018, **9**, 4523–4534, DOI: 10.1039/C8PY01031E.

12 Y. C. Chen, S. Y. Fu and H. Zhang, Signally improvement of polyurethane adhesive with hydroxy-enriched lignin from

bagasse, *Colloids Surf., A*, 2020, **585**, 124164, DOI: 10.1016/j.colsurfa.2019.124164.

13 M. Liu, Z. Y. Wang, P. Liu, Z. K. Wang, H. M. Yao and X. Yao, Supramolecular silicone coating capable of strong substrate bonding, readily damage healing, and easy oil sliding, *Sci. Adv.*, 2019, **5**, 5643, DOI: 10.1126/sciadv.aaw5643.

14 J. Liu, C. S. Y. Tan, Z. Y. Yu, N. Li, C. Abell and O. A. Scherman, Tough supramolecular polymer networks with extreme stretchability and fast room-temperature self-healing, *Adv. Mater.*, 2017, **29**, 1605325, DOI: 10.1002/adma.201605325.

15 G. Weng, S. Thanneeru and J. He, Dynamic coordination of Eu-iminodiacetate to control fluor Chromic response of polymer hydrogels to multistimuli, *Adv. Mater.*, 2018, **30**, 1706526, DOI: 10.1002/adma.201706526.

16 M. Bednarek and P. Kubisa, Reversible networks of degradable polyesters containing weak covalent bonds, *Poly. Chem.*, 2019, **10**(15), 1848–1872, DOI: 10.1039/C8PY01731J.

17 T. Defize, J. Thomassin, M. Alexandre, B. Gilbert, R. Riva and C. Jerome, Comprehensive study of the thermo-reversibility of Diels-Alder based PCL polymer networks, *Polymer*, 2016, **84**, 234–242, DOI: 10.1016/j.polymer.2015.11.055.

18 M. Y. Wu, Y. Liu, P. F. Du, X. L. Wang and B. Yang, Polyurethane hot melt adhesive based on Diels-Alder reaction, *Int. J. Adhes. Adhes.*, 2020, **100**, 102597, DOI: 10.1016/j.ijadhadh.2020.102597.

19 T. Defize, R. Riva, C. Jerome and M. Alexandre, Multifunctional poly(ε-caprolactone)-forming networks by Diels–Alder cycloaddition: Effect of the adduct on the shape-memory properties, *Macromol. Chem. Phys.*, 2012, **213**(2), 187–197, DOI: 10.1002/macp.201100408.

20 D. H. Turkenburg, E. Gavin, O. Jones and K. N. Houk, Conceptual, qualitative, and quantitative theories of 1,3-Dipolar and Diels–Alder cycloadditions used in synthesis, *Adv. Synth. Catal.*, 2006, **348**(16-17), 2337–2361, DOI: 10.1002/adsc.200600431.

21 D. H. Turkenburg, Y. Durant and H. R. Fischer, Bio-based self-healing coatings based on thermo-reversible Diels-Alder reaction, *Prog. Org. Coat.*, 2017, **111**, 38–46, DOI: 10.1016/j.porgcoat.2017.05.006.

22 S. Y. Cai, Z. Qiang, C. Zeng and J. Ren, Multifunctional poly(lacticacid) copolymers with room temperature self-healing and rewritable shape memory properties *via* Diels-Alder reaction, *Mater. Res. Express*, 2019, **6**, 045701, DOI: 10.1088/2053-1591/aafba3.

23 A. M. Peterson, R. E. Jensen and G. R. Palmese, Room-Temperature healing of a thermosetting polymer using the Diels-Alder Reaction, *ACS Appl. Mater. Interfaces*, 2010, **2**(4), 1141, DOI: 10.1021/am9009378.

24 D. H. Turkenburg and H. R. Fischer, Diels-Alder based, thermo-reversible cross-linked epoxies for use in self-healing composites, *Polymer*, 2015, **79**(19), 187, DOI: 10.1016/j.polymer.2015.10.031.

25 C. H. Lin, D. K. Sheng, X. D. Liu, S. Xu and Y. Yang, Effect of different sizes of graphene on Diels-Alder self-healing polyurethane, *Polymer*, 2019, **182**(7), 121822, DOI: 10.1016/j.polymer.2019.121822.

26 D. K. Owens and R. C. Wendt, Estimation of the surface free energy of polymers, *J. Appl. Polym. Sci.*, 1969, **13**, 1741–1747, DOI: 10.1002/app.1969.070130815.

27 E. E. Kahveci and T. Imdat, Experimental study on performance evaluation of PEM fuel cell by coating bipolar plate with materials having different contact angle, *Fuel*, 2019, **253**, 1274–1281, DOI: 10.1016/j.fuel.2019.05.110.

28 J. H. Aubert, Thermally removable epoxy adhesives incorporating thermally reversible diels-alder adducts, *J. Adhes.*, 2003, **79**, 609–616, DOI: 10.1080/00218460309540.

29 A. J. Inglis, L. Nebhani, O. Altintas, F. G. Schmidt and C. Barner-Kowollik, Rapid Bonding/Debonding on Demand: Reversibly Cross-Linked Functional Polymers *via* Diels–Alder Chemistry, *Macromolecules*, 2010, **43**, 5515–5520, DOI: 10.1021/ma100945b.

30 J. J. Park and K. G. Yoon, Thermal and mechanical properties of epoxy/Micro- and nano-mixed silica composites for insulation materials of heavy electric equipment, *IEEJ Trans. Electr. Electron. Eng.*, 2011, **2**, 98–101, DOI: 10.4313/TEEM.2011.12.3.98.

31 N. E. Kochkina and O. A. Butikova, Effect of fibrous TiO_2 filler on the structural, mechanical, barrier and optical characteristics of biodegradable maize starch/PVA composite films, *Int. J. Biol. Macromol.*, 2019, **139**, 431–439, DOI: 10.1016/j.ijbiomac.2019.07.213.

32 T. Rettelbach, J. Sauberlich, S. Korder and J. Fricke, Thermal conductivity of silica aerogel powders at temperatures from 10 to 275 K, *J. Non-Cryst. Solids*, 1995, **186**, 278–284, DOI: 10.1016/0022-3093(95)00051-8.

33 A. Allahverd, M. Ehsani, H. Janpour and S. Ahmadi, The effect of nanosilica on mechanical, thermal and morphological properties of epoxy coating, *Prog. Org. Coat.*, 2012, **75**, 543–548, DOI: 10.1016/j.porgcoat.2012.05.013.

34 W. Hong, M. W. Meng, J. L. Xie, D. D. Gao, M. N. Xian, S. Wen, S. Y. Huang and C. Y. Kang, Properties and thermal analysis study of modified polyvinyl acetate (PVA) adhesive, *J. Adhes. Sci. Technol.*, 2018, **32**(19), 2180–2194, DOI: 10.1080/01694243.2018.1465687.

35 E. Espinosa, I. Bascón-Villegas, A. Rosal, F. Pérez-Rodríguez, G. Chinga-Carrasco and A. Rodríguez, PVA/(ligno) nanocellulose biocomposite films. Effect of residual lignin content on structural, mechanical, barrier and antioxidant properties, *Int. J. Biol. Macromol.*, 2019, **141**, 197–206, DOI: 10.1016/j.ijbiomac.2019.08.262.

36 X. Zhang, W. Liu, W. Liu and X. Qiu, High performance PVA/lignin nanocomposite films with excellent water vapor barrier and UV-shielding properties, *Int. J. Biol. Macromol.*, 2020, **142**, 551–558, DOI: 10.1016/j.ijbiomac.2019.09.129.

37 H. Lee, J. You, H. Jin and H. W. Kwak, Chemical and physical reinforcement behavior of dialdehyde nanocellulose in PVA composite film: a comparison of nanofiber and nanocrystal, *Carbohydr. Polym.*, 2020, **232**, 115771, DOI: 10.1016/j.carbpol.2019.115771.